31st Annual International Conference of the IEEE EMBS
Minneapolis, Minnesota, USA, September 2-6, 2009

Catheter Localization in the Left Atrium using an Outdated Anatomic Reference for Guidance

Aditya B. Koolwal Federico Barbagli Christopher R. Carlson David H. Liang

***Abstract*— We present a method for registering real-time ultrasound of the left atrium to an outdated, anatomic surface mesh model, whose shape differs from that of the anatomy. Using an intracardiac echo (ICE) catheter with mounted 6DOF electromagnetic position/orientation sensor (EPS), we acquire images of the left atrium and determine where the ICE catheter must be positioned relative to the surface mesh to generate similar, "virtual" ICE images. Further, we use an affine warping model to infer how the shape of the surface mesh differs from that of the atrium.**

Our registration and warping algorithm allows us to display EPS-sensorized catheters inside the surface mesh, facilitating guidance for left atrial procedures. By solving for the atrium-to-mesh warping parameters, we ensure that tissue contact in the anatomy is properly displayed as tissue contact in the mesh.

After considering less than thirty seconds worth of ICE data, we are able to accurately localize EPS measurements within the surface mesh, despite surface mesh warpings of up to $\pm 20\%$ along and about the principal axes of the left atrium. Further, because our estimation framework is iterative and continuous, our accuracy improves as new data is acquired.

***Index Terms*— ablation catheter, guidance, left atrium, ultrasound, particle filter**

I. Introduction

The treatment of atrial fibrillation by means of catheter ablation allows physicians to operate inside the atria without having to perform open heart surgery. Unfortunately, this procedure can be very time-consuming, as traditional imaging modalities fail to yield a clear and comprehensive picture of the surgical environment. To overcome this visualization hurdle, physicians often rely on electromagnetic position/orientation sensors (EPS) to record the 3D position and orientation of the ablation catheter's tip as it moves inside the atria. In [1] we proposed a method for registering EPS measurements to a CT/MR-based anatomic surface mesh, facilitating guidance by allowing EPS-tracked devices to be displayed inside the surface mesh.

Figure 1 illustrates our registration algorithm. Briefly, we mount an EPS sensor to the tip of an ICE catheter to track its *pose* (position and orientation) during intracardiac imaging, and simulate "virtual" ICE images of the surface mesh based on measured changes in pose. By comparing virtual images to acquired images, we determine how the ICE catheter is positioned with respect to the anatomy. We then use the ICE catheter's EPS measurement to compute the transformation between EPS and anatomic coordinates. In [1] we demonstrated convergence in estimating accurate registration parameters after considering less than thirty second's worth of acquired ICE data.

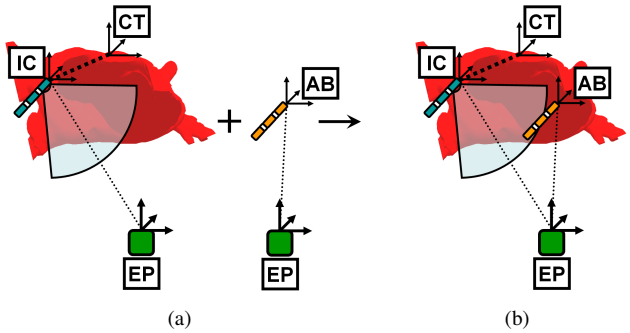

Fig. 1. Registering EPS Measurements to an Anatomic Surface Mesh. In (a) we assign reference frames to the EPS reference electrode (*EP*), ICE catheter tip (*IC*), ablation catheter tip (*AB*), and CT/MR-based surface mesh (*CT*). Using an EPS sensor mounted to the tip of the ICE catheter, we measure the transformation between *EP* and *IC*. We then employ an ultrasound-to-surface-mesh registration algorithm described in [1] to estimate the transformation between *IC* and *CT*. Finally, we compute the transformation between *EP* and *CT* using our measurements and estimates. Finally, we display the EPS-tracked ablation catheter inside the mesh (b).

One deficiency of this algorithm is that it assumes the shape of the surface mesh closely matches that of the anatomy. This assumption is reasonable because typically, prior to undergoing a catheter ablation procedure, a patient will have a CT study taken, so the data used to reconstruct the mesh is that of the patient's anatomy. However, in the time between the CT study and the procedure, the shape of the anatomy may vary for reasons ranging from disease progression, to how the patient lies on the operating room table. In practice, a surface mesh generated from a pre-operative CT is "out-of-date" by the time the procedure starts; while its overall structure still resembles that of the anatomy, slight variations may negatively impact our ability to indicate tissue contact when displaying EPS measurements inside the mesh.

II. Contributions

In this paper we relax the assumption that the surface mesh and imaged anatomy are identically shaped. We augment the algorithm described in [1] to additionally solve for a set of warping parameters that estimate the morphological differences between the surface mesh and the left atrium. These warping parameters are used to shift EPS measurements so

A.B. Koolwal is with the Department of Mechanical Engineering, Stanford University, Stanford, CA, USA
F. Barbagli is with the Department of Computer Science, Stanford University, Stanford, CA, USA
C.R. Carlson is with Hansen Medical, Inc., Mountain View, CA, USA
D.H. Liang is with the Department of Cardiovascular Medicine, Stanford University, Stanford, CA, USA

their positioning relative to the tissue surface is the same in the surface mesh as it is within the anatomy. We use ICE ultrasound to aid in estimating these warping parameters.

Because automatically identifying features in left atrial ICE data is difficult, we must extract additional information from our ICE catheter pose estimate to assess how the shape of the anatomy differs from the shape of the surface mesh. While we continue to estimate the global registration parameters linking EPS coordinates to anatomy coordinates, we also estimate a set of local registration parameters that describe the additional "nudge" needed to position the ICE catheter correctly inside the surface mesh (Figure 2). With this additional information, we can compute how to transform anatomically-registered coordinates into the surface mesh reference frame, and vice-versa, without affecting the run-time performance of our algorithm. This allows us to estimate and visualize tissue surface contact without requiring additional instrumentation of the ablation catheter – such as mounting a contact sensor to its tip – which would increase the complexity and cost of catheter production.

III. Methods

A. Reference Frame Notation

We codify our knowledge of state using the reference frames show in Figure 1. We relate reference frames A and B with transformation matrix $T \in \mathbb{R}^{4\times4}$:

$$ {}^{A}T^{B} = \begin{bmatrix} {}^{A}R^{B} & {}^{A}O^{B} \\ 000 & 1 \end{bmatrix} \tag{1} $$

where ${}^{A}R^{B} \in \mathbb{R}^{3\times3}$ and ${}^{A}O^{B} \in \mathbb{R}^{3\times1}$ are the rotation and origin offsets between A and B's coordinate axes. We represent ${}^{A}T^{B}$ by its pose vector ${}^{A}P^{B} \in \mathbb{R}^{6\times1}$:

$$ {}^{A}P^{B} = [x, y, z, \alpha, \beta, \gamma]^{T} \tag{2} $$

where ${}^{A}O^{B} = [x, y, z]^{T}$ and α, β, and γ are the xyz Euler angles used to compute ${}^{A}R^{B}$. Finally, we define function $h_{P\rightarrow T} \in \mathbb{R}^{6\times1\rightarrow4\times4}$ to convert ${}^{A}P^{B}$ into ${}^{A}T^{B}$, with corresponding inverse $h_{T\rightarrow P} \in \mathbb{R}^{4\times4\rightarrow6\times1}$.

B. Recursive Bayesian State Estimation

Our incremental registration algorithm transforming EPS measurements into anatomic coordinates relies on a Recursive Bayesian State Estimation (RBSE) framework. At time step k, the RBSE state estimate is defined as the *posterior* distribution of state $\mathbf{x}_k$ conditioned on all past controls $\mathbf{u}_{1:k}$ and measurements $\mathbf{z}_{1:k}$ ([2]):

$$ f_{est}(\mathbf{x}_k) = p(\mathbf{x}_k \,|\, \mathbf{u}_{1:k}, \mathbf{z}_{1:k}) \tag{3} $$

Here, state variable $\mathbf{x}$ is the pose of the ICE catheter with respect to the surface mesh:

$$ \mathbf{x}_k = {}^{CT}P_{est}^{IC_k} \tag{4} $$

We define control variable $\mathbf{u}$ to be the change in pose of the ICE catheter tip between times $k-1$ and k:

$$ \mathbf{u}_k = h_{T\rightarrow P}\left(\left({}^{IC_{k-1}}T_{meas}^{EP}\right)\left({}^{EP}T_{meas}^{IC_k}\right)\right) \tag{5} $$

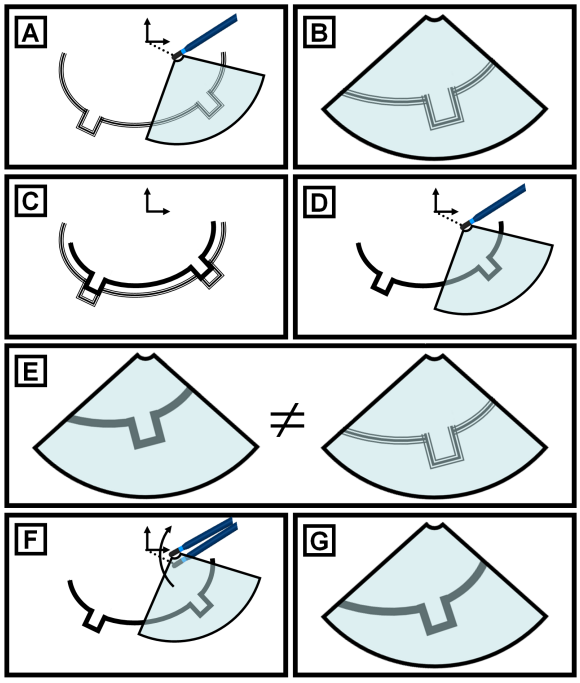

Fig. 2. Local Registration. In (A) we see the ICE catheter imaging the surface of the left atrium (triple line), and in (B) we see the acquired ICE image. In (C) we overlay the reference surface mesh (solid line) on top of the left atrium to demonstrate their differences in morphology. In (D) we position the ICE catheter inside the surface mesh identically to its positioning in (A), and simulate a virtual ICE image of the surface mesh. Unfortunately, this virtual image (E) does not match the acquired ICE image. In (F) we "nudge" the catheter into a position that is more well suited for simulating a virtual ICE image which better-matches the acquired ICE image (G). The local registration parameters for the catheter configuration shown in (A) are equivalent to this nudge.

where ${}^{EP}T_{meas}^{IC_{k-1}}$ and ${}^{EP}T_{meas}^{IC_k}$ are the last two EPS measurements of the ICE catheter's pose.

Finally, the acquired $n \times m$ ICE image serves as our measurement variable $\mathbf{z}_k \in \mathbb{R}^{n\times m}$. Our measurement estimate, $\mathbf{y}_k \in \mathbb{R}^{n\times m}$, is a virtual ICE image generated by sampling planar cross-sections of the reference surface mesh. The planar cross-section is filtered using a simplified model for ultrasound reflections. Acquired ICE image $\mathbf{z}_k$ is compared to $\mathbf{y}_k$ using a normalized mutual information (NMI) correlation metric defined in [3]. Please refer to [1] for more details regarding this algorithm.

C. Registration Parameter Estimation

To estimate the warping parameters that model the differences in shape between the surface mesh and the left atrium, we first compute global transformation matrix ${}^{LA}T_{glob}^{EP_k}$, which maps EPS measurements into the left atrium reference frame (LA) , then compute local transformation matrix ${}^{CT}T_{loc}^{LA}$, which maps LA coordinates into the CT reference frame. This is achieved using EPS measurements and RBSE estimates of the ICE catheter's pose:

$$ {}^{CT}T_{est}^{IC_k} = \left({}^{CT}T_{loc}^{LA}\right)\left({}^{LA}T_{glob}^{EP_k}\right)\left({}^{EP_k}T_{meas}^{IC_k}\right) \tag{6} $$

We approximate ${}^{LA}T_{glob}^{EP_k}$ using least-squares by considering the last n EPS measurements and RBSE estimates simultaneously. For this approach to be valid, we must assume that the *CT* and *LA* reference frames are co-located, and that warping is symmetric about their coordinate origin. Further, we must ensure that the last n catheter poses are distributed symmetrically around the origin. If these conditions are met, the average local warping contribution over all poses should approach zero. Once we have collected enough data to estimate ${}^{LA}T_{glob}^{EP_k}$ with reasonable certainty, we can recover ${}^{CT}T_{loc}^{LA}$ from Eqn. 6 for ensuing pose measurements.

D. Warping Parameter Estimation

Next, we use ${}^{CT}T_{loc}^{LA}$ to estimate how the surface of the reference mesh should be transformed to better match the surface of the anatomy. We define $S^{CT} = \{S_0^{CT}, S_1^{CT}, \ldots, S_N^{CT}\}$ to be the set of points $S_i^{CT} = \begin{bmatrix} S_{i_x}^{CT} & S_{i_y}^{CT} & S_{i_z}^{CT} \end{bmatrix}^T \in \mathbb{R}^3$ lying on the surface of the mesh, and $S^{LA} = \{S_0^{LA}, S_1^{LA}, \ldots, S_N^{LA}\}$ to be the set of points lying on the surface of the left atrium. A carefully segmented and stitched volume of ultrasound images would yield an estimate of S^{LA}, but this would require a fairly sophisticated segmentation algorithm that could reliably distinguish left atrium wall reflections from other signal content in the acquired ICE images. Instead we choose to estimate S^{LA} by warping S^{CT}; we assume there exists some warping function $W \in \mathbb{R}^{3\times3}$ that transforms each S_i^{CT} into S^{LA}, and whose inverse, W^{-1}, transforms each S_i^{LA} into S^{CT}. More generally, W^{-1} takes EPS measurements of the ablation catheter in the left atrium and displays them properly inside the surface mesh.

We assume that W is an affine matrix of the form:

$$W = \begin{bmatrix} 1+w_{xx} & w_{xy} & w_{xz} \\ 0 & 1+w_{yy} & w_{yz} \\ 0 & 0 & 1+w_{zz} \end{bmatrix} \tag{7}$$

where $1+w_{ii}$ measures the amount of stretching along the i axis, and w_{ij} measures the amount of shearing on the ij plane (about the k axis). To determine a least-squares estimate of the w_{ii} and w_{ij}, we need at least $M \geq 6$ corresponding $\left(S_i^{CT}, S_i^{LA}\right)$ surface points. However, because we cannot reliably identify landmarks in our acquired ICE images, generate such a set of corresponding points is a difficult task.

Instead, we discretize the volume subsuming the surface mesh into a series of sub-volumes, where the center of each sub-volume is used as a makeshift landmark. For each ICE catheter pose estimate, we identify the sub-volumes containing points that appear in the corresponding virtual ICE image, and apply $\left({}^{CT}T_{loc}^{LA}\right)^{-1}$ to each "touched" sub-volume (Figure 3). Our rationale is that these sub-volumes should theoretically move back towards the "pre-nudged" ICE catheter configuration to better match the true shape of the anatomy. Once we have imaged a sufficient portion of the anatomy, we can compute W for the entire volume by considering all of the $\left({}^{CT}T_{loc}^{LA}\right)^{-1}$ transformations applied to sub-volumes "touched" over the last m time steps.

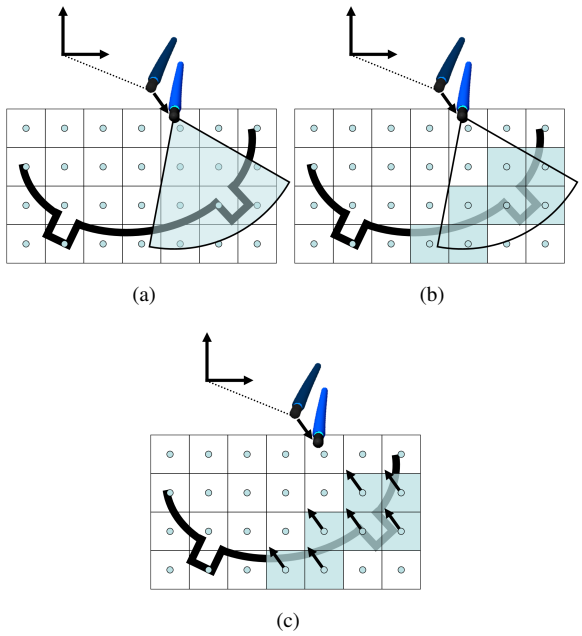

Fig. 3. Warping Parameter Estimation. In (a) we see the volume surrounding the surface mesh discretized into sub-volumes, the original and "nudged" catheter configurations, and the virtual ICE image acquired from the final pose estimate. In (b) we identify the sub-volumes "touched" by the virtual ICE image, and in (c) we apply the inverse of the transformation used to nudge the catheter to each of the touched sub-volumes.

IV. Results

To evaluate the performance of our algorithm, we first warp a CT-based left atrium surface mesh along and about its three principal axes, namely: the anterior-posterior (AP), medial-lateral (ML), and inferior-superior (IS) axes. Then we collect a series ICE ultrasound images inside a left atrium ultrasound phantom, while simultaneously updating our registration parameter estimates using the warped surface mesh model as a basis for comparison.

A. Surface Mesh and Phantom Generation

We generate the surface mesh by segmenting the left atrium from a cardiac CT scan using Verizmo (*St. Jude Medical, Minneapolis, MN*), a software platform for CT segmentation widely-employed in EP medicine.

To test our algorithm *in vitro*, we created an ultrasound phantom using the surface mesh as a geometric reference. The phantom is a cavity-mold cast in 0.1% silicone dioxide, a composite material that exhibits tissue-like reflectivity when imaged under ultrasound. The surface of the cavity-mold was bead-blasted to generate texture for improved reflections.

B. Ultrasound Acquisition and Calibration

A 6DOF position/orientation sensor (*Ascension Technologies, Burlington, VT*) is affixed to both the ICE catheter tip and the ultrasound phantom, so that at all points in time we know the pose of the ICE catheter relative to the phantom. We determined the transformation relating ICE pixels to sensor coordinates using a single-target calibration phantom described in [1].

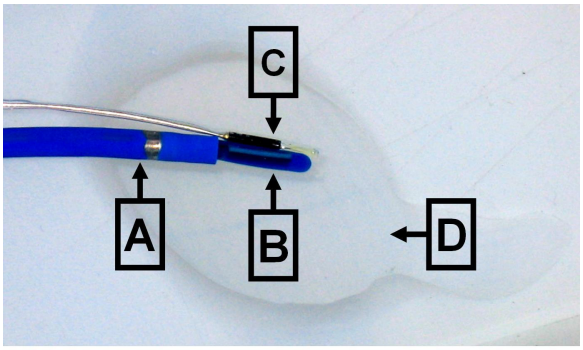

Fig. 4. ICE Acquisition of Ultrasound Phantom. The ICE catheter is run up through a sheath (A) for stability, and its tip emerges from the sheath's lumen (B). A sensor (C) is mounted to the ICE catheter's tip for validation measurements. The ICE catheter images a left atrium phantom (D) serving as an anatomical proxy.

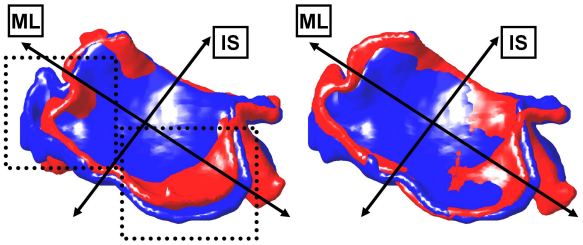

(a) (b)

Fig. 5. Surface Mesh Unwarping. In (a) we see a warped surface mesh (light red) overlaid on top of the actual left atrium surface (dark blue). There are significant disparities between the surfaces along both the ML and IS axes. In (b) we see the unwarped surface mesh (light red) generated using global registration and warping parameter estimates. While the unwarped mesh does not entirely match the left atrium's surface (dark blue), the disparities between the two are substantially less than those observed in (a).

The ultrasound phantom is submerged in a water bath and an AcuNav ICE catheter (*Siemens Ultrasound, Mountain View, CA*) is manually positioned inside the phantom for imaging (Figure 4). The ICE catheter is attached to a Sequoia Ultrasound System (*Siemens Ultrasound, Mountain View, CA*), whose output images are frame-grabbed onto a PC using a Foresight I-Color frame-grabber (*Foresight, Boston, MA*) at a rate of $15Hz$.

C. Surface Mesh Unwarping

We evaluate the performance of our estimation algorithm over a number of trials using data-sets collected by rotating the ICE catheter axially to image a swept volume of the ultrasound phantom. The ICE catheter's handle is attached to a mechanical rotator, which applies a $0.1Hz$, 60° sine-wave trajectory for three cycles. Prior to running each trial, we compute W_{act} by randomly setting its w_{ii} and w_{ij} parameters to values within the range of ± 0.2, and warp the reference surface mesh using W_{act}^{-1}.

The EPS sensor mounted to the phantom allows us to measure ${}^{EP}T^{CT}$, which can be used to compute ${}^{EP}T^{S_i^{CT}}$ for each point on the warped surface mesh. At the end of each trial, we use the final estimates of ${}^{LA}T_{glob}^{EP}$ and W_{est} to approximate S^{LA} by unwarping the S_i^{CT} as follows:

$$ {}^{LA}T_{est}^{S_i^{LA}} = \left(W_{est}\right)\left({}^{LA}T_{glob}^{EP}\right)\left({}^{EP}T^{S_i^{CT}}\right) \tag{8} $$

We assess the error in our unwarped surface approximation by computing the Euclidean distance between each of the ${}^{LA}T_{est}^{S_i^{LA}}$ and ${}^{LA}T_{act}^{S_i^{LA}}$, where:

$$ {}^{LA}T_{act}^{S_i^{LA}} = \left(W_{act}\right)\left({}^{LA}T^{S_i^{CT}}\right) \tag{9} $$

Over all trials performed, the average point-to-point error between the unwarped S_{est}^{LA} and S_{act}^{LA} was $0.544mm$, while the average point-to-point error between the warped S^{CT} and S^{LA} was $2.815mm$. Because the AP and IS axes are approximately $50mm$ in length, and because the *LA* reference frame origin is assumed to be in the geometric center of the atrium, the expected point-to-point error between S^{CT} and S^{LA} is approximately $\frac{50mm}{2} \times \frac{0.2}{2} = 2.5mm$, where $\frac{0.2}{2}$ is the average warping parameter magnitude. Our observed errors indeed fall in line with this expectation.

In Figure 5 we show the surface of the left atrium overlaid on top of a warped mesh taken from the beginning of a trial (Figure 5(a)), and the unwarped mesh estimated at the end of the trial (Figure 5(b)). The unwarped mesh has greater overlap with the left atrium, indicating that tissue contact would be better displayed in the reference mesh by transforming EPS measurements using W_{est}.

V. Discussion

We have presented a method for registering EPS data to a reference surface mesh of the left atrium for improved guidance in the catheter ablation procedure. In addition to estimating the registration parameters converting EPS measurements into anatomic coordinates, we also estimate changes in shape between the anatomy and the reference mesh. In doing so, we aim to ensure that when a catheter touches tissue in the anatomy, contact is properly displayed on the surface of the reference mesh, even if its shape differs from that of the anatomy.

After considering less than thirty second's worth of acquired ICE data, we are able to estimate tissue contact to within $\approx 0.5mm$ of accuracy, even when the anatomy deviates from the reference mesh by $\approx 3mm$. In the future, we plan to leverage the algorithms developed in this study to continuously warp the reference mesh so it better fits acquired EPS measurements, rather than warping measurements to better fit the mesh. We also intend to modify our framework to enable elastic reference frame warping by simltaneously considering the "nudges" applied to all sub-volumes "touched" during imaging.

References

[1] A. B. Koolwal, F. Barbagli, C. R. Carlson, and D. H. Liang, "An ultrasound-based localization algorithm for catheter ablation guidance in the left atrium," *The International Journal of Robotics Research*, 2009.

[2] S. Thrun, "Probabilistic algorithms in robotics," *AI Magazine*, vol. 21, no. 4, pp. 93–109, 2000.

[3] J. P. Pluim, J. A. Maintz, and M. A. Viergever, "Mutual-information-based registration of medical images: A survey," *IEEE Transactions on Medical Imaging*, vol. 22, no. 8, pp. 986–1004, 2003.